NASA TECHNICAL NOTE

NASA TN D-8095

NASA TN D-8095

EFFECTS OF LONG-TERM AGING ON DUCTILITY OF THE COLUMBIUM ALLOYS C-103, Cb-1Zr, AND Cb-752 AND THE MOLYBDENUM ALLOY Mo-TZM

Joseph R. Stephens

Lewis Research Center

Cleveland, Ohio 44135

NATIONAL AERONAUTICS AND SPACE ADMINISTRATION • WASHINGTON, D. C. • OCTOBER 1975

1. Report No. NASA TN D-8095	2. Government Accession No.	3. Recipient's Catalog No.
4. Title and Subtitle EFFECTS OF LONG-TERM AGING ON DUCTILITY OF THE COLUMBIUM ALLOYS C-103, Cb-1Zr, AND Cb-752 AND THE MOLYBDENUM ALLOY Mo-TZM		5. Report Date October 1975
		6. Performing Organization Code
7. Author(s) Joseph R. Stephens		8. Performing Organization Report No. E-8374
		10. Work Unit No. 506-16
9. Performing Organization Name and Address Lewis Research Center National Aeronautics and Space Administration Cleveland, Ohio 44135		11. Contract or Grant No.
		13. Type of Report and Period Covered Technical Note
12. Sponsoring Agency Name and Address National Aeronautics and Space Administration Washington, D.C. 20546		14. Sponsoring Agency Code
15. Supplementary Notes		

16. Abstract

A program was conducted to determine if aging embrittlement occurs in the columbium alloys C-103, Cb-1Zr, and Cb-752 or in the molybdenum alloy Mo-TZM. Results showed that aging embrittlement does not occur in C-103, Cb-1Zr, or Mo-TZM during long-term (1000 hr) aging at temperatures in the range 700° to 1025° C. In contrast, aging embrittlement did occur in the Cb-752 alloy after similar aging at 900° C. A critical combination of the solute additions W and Zr in Cb-752 led to Zr segregation at grain boundaries during long-term aging. This segregation subsequently resulted in embrittlement as indicated by an increase in the ductile-brittle transition temperature from below -196° C to about -150° C.

17. Key Words (Suggested by Author(s)) Columbium; Molybdenum; Aging embrittlement; Hydrogen embrittlement; Ductility	18. Distribution Statement Unclassified - unlimited STAR category 26 (rev.)

19. Security Classif. (of this report)	20. Security Classif. (of this page)	21. No. of Pages	22. Price*
Unclassified	Unclassified	25	$3.25

* For sale by the National Technical Information Service, Springfield, Virginia 22161

CONTENTS

EFFECTS OF LONG-TERM AGING ON DUCTILITY OF THE COLUMBIUM ALLOYS C-103, Cb-1Zr, AND Cb-752 AND THE MOLYBDENUM ALLOY Mo-TZM

by Joseph R. Stephens

Lewis Research Center

SUMMARY

Columbium and molybdenum alloys have potential application in space power systems. Therefore, a program was conducted to determine if aging embrittlement occurs in these alloys and also to determine if aging embrittlement of columbium alloys is dependent on alloy composition. Alloys investigated included C-103, the primary candidate alloy for structural applications in a current space power system, plus an alternate alloy, Cb-1Zr. Also included in the investigation were Cb-752 and a molybdenum alloy, Mo-TZM. Alloy specimens were aged for 1000 hours at five temperatures in the range 700° to 1025° C. The bend ductile-brittle transition temperature and metallographic characterization were used as the primary methods of evaluation. Aged specimens subsequently doped with hydrogen also were bend tested to determine if aging increases the sensitivity of Cb and Mo alloys to hydrogen embrittlement.

The results showed that the Cb alloy C-103 is not susceptible to aging embrittlement. Specimens in the aged condition and even those doped with hydrogen exhibited a ductile-brittle transition temperature below -196° C. The Cb-1Zr and Mo-TZM alloys also did not exhibit aging embrittlement. Hydrogen doping of aged Cb-1Zr specimens, however, produced an increase in the ductile-brittle transition temperature to -100° C, compared to less than -196° C for the undoped, aged material. The aged Mo-TZM alloy could not be doped with hydrogen.

Conversely, long-term aging at 900° C produced some aging embrittlement in the Cb-752 alloy. This was indicated by an increase in the ductile-brittle transition temperature (from below -196° C to about -150° C). Embrittlement was attributed to a critical combination of solute additions of W and Zr in this alloy. It was shown by light microscopy that, during aging, Zr segregation to grain boundaries occurs. This segregation leads to subsequent brittle failure along the grain boundaries. The Cb-752 alloy also was susceptible to hydrogen embrittlement. Annealed and aged specimens doped with approximately 40 ppm hydrogen had transition temperatures above room temperature.

INTRODUCTION

Columbium (Cb) and molybdenum (Mo) alloys are used as structural members in space power systems where stress, time, temperature, and environmental conditions preclude the use of iron (Fe), nickel (Ni), and cobalt (Co) base alloys. The advantages of Cb and Mo alloys include their high creep resistance and their microstructural stability during operation for several thousand hours at elevated temperatures in a high-vacuum space environment. In addition, Cb alloys possess excellent low-temperature ductility and fabricability. Columbium alloys are currently being considered for structural applications in a multihundred-watt radioisotope-turbogenerator space power system (ref. 1). Long-term, high-vacuum operation will be required over the temperature range 700° to 1025° C. On a homologous temperature basis for Cb alloys, this temperature range corresponds to 0.36 to 0.47 T_m, where T_m is the absolute melting temperature. Similarly, for Mo alloys, which may find applications over a similar temperature range, 700° to 1025° C corresponds to a homologous temperature range of 0.34 to 0.45 T_m. Previous results with tantalum (Ta) alloys (refs. 2 to 5) have shown that long-term aging near 0.4 T_m can result in subsequent near-room-temperature embrittlement and increased sensitivity to hydrogen embrittlement.

The primary purposes of this investigation were (1) to determine if aging embrittlement occurs in Cb alloys and an Mo alloy under the conditions expected in space power systems and (2) to determine if aging embrittlement, especially in Cb alloys, is dependent upon alloy composition. The author (ref. 5) has shown alloy composition to be the controlling mechanism for aging embrittlement in Ta alloys. Four alloys were included in the current investigation. Two of the Cb alloys investigated are being considered for structural applications in a multihundred-watt, radioisotope-turbogenerator power system. This system is to serve as the electrical power source for a wide range of space missions involving long-life performance - 5 to 10 years. The primary alloy is C-103 (Cb - 10 hafnium (Hf) - 1 titanium (Ti)),[1] and the alternate alloy is Cb - 1 zirconium (Zr). Also included in the current program was Cb-752 (Cb - 10 tungsten (W) - 3 Zr). This columbium alloy is postulated to exhibit aging embrittlement based on its critical combination of W and Zr, in a manner analogous to embrittlement in Ta alloys containing W and Hf (ref. 5). The fourth alloy investigated was a widely used Mo-base alloy, Mo-TZM (Mo-0.5Ti-0.1Zr). The combination of an Mo matrix and the reactive element Zr in this alloy suggests that aging embrittlement may be a possibility.

The four alloys were aged for 1000 hours at temperatures from 700° to 1025° C. This temperature range encompasses the homologous temperature range that has been observed to produce aging embrittlement and increased sensitivity to hydrogen embrittlement in Ta alloys (ref. 4). Alloys were evaluated after the 1000-hour aging treatments

---

[1]Nominal compositions are in weight percent unless stated otherwise.

by means of bend tests, light metallography, and scanning electron microscopy. After aging, some of the specimens were doped with hydrogen and then evaluated.

EXPERIMENTAL PROCEDURE

Materials

The chemical compositions of the alloys evaluated in this study are listed in table I. The alloys were obtained in the form of sheet approximately 0.75 millimeter thick. Longitudinal bend specimens 6.4 millimeters by 25.4 millimeters were cut from each of the alloy sheets. A standard annealing treatment of 1 hour at 1345° C (0.59 T_m) in a vacuum of 0.13 $\mu N/m^2$ was used for each of the Cb alloys. The Mo-TZM alloy was vacuum annealed at an equivalent homologous temperature, 1425° C.

Aging

Aging consisted of heating the bend specimens at a temperature in the range 700° to 1025° C for 1000 hours in a vacuum of 0.13 $\mu N/m^2$. Table II lists the five aging temperatures that were used for each alloy. Specimens were weighed before and after aging. They were analyzed for interstitial impurity content after aging to determine if contamination occurred during the aging treatment. No significant changes in weight or interstitial impurity content resulted from the 1000-hour vacuum aging treatment.

Hydrogen Doping

Three annealed specimens and four aged specimens from each of the five aging treatments for each alloy were doped with hydrogen to determine if aging increases the sensitivity to hydrogen embrittlement in the Cb and Mo alloys that were investigated. Hydrogen doping was attempted by heating the specimens in an evacuated furnace to a temperature of 825° C. At this point, hydrogen was introduced into the furnace to a pressure of 13 kN/m^2. Specimens were held in hydrogen under these conditions for 10 minutes and then cooled to room temperature in a helium atmosphere.

Evaluation

Bend tests. - Bend testing was used as the primary means of determining the effects of aging on the Cb and Mo alloys. Tests were conducted in a screw-driven testing machine at a punch rate of approximately 25 millimeters per minute. A bend radius of 2t, where t is equal to the specimen thickness, and a maximum total bend angle of about 140° were used for all tests. Tests were conducted over the temperature range -196° to 1000° C. A controlled liquid-nitrogen spray was used for tests below room temperature. For tests above room temperature, a clam-shell infrared furnace was employed. The bend ductile-brittle transition temperature, defined in this study as the lowest temperature at which a specimen could successfully complete the 140° bend angle, was determined for each alloy in the annealed, aged, and hydrogen-doped conditions.

Metallography. - Specimens from each alloy in the annealed and aged conditions were examined by standard light microscopy techniques to determine aging effects on grain size and general structure. Fracture surfaces of selected specimens from each alloy were characterized by scanning electron microscopy.

RESULTS

Bend Ductility of Annealed and Aged Alloys

Bend tests were conducted on specimens of C-103, Cb-1Zr, Cb-752, and Mo-TZM in the annealed condition and after aging for 1000 hours at temperatures from 700° to 1025° C to determine if aging embrittlement occurred. The bend ductile-brittle transition temperatures (DBTT) are summarized in table II. The bend test results are compared in figure 1 for each of the four alloys. The bend ductilities (figs. 1(a) and (b)) for the two Cb alloys that are being considered for current space power systems, C-103 and Cb-1Zr, were not impaired as a result of aging over the critical (refs. 3 and 4) homologous temperature range 0.35 to 0.47 T_m. The DBTT for these two alloys in the annealed and aged conditions was at least -196° C, the lowest test temperature attainable by the test facility used in this study.

In contrast to the results for C-103 and Cb-1Zr, aging the Cb-752 alloy (fig. 1(c)) at 900° C (0.43 T_m) resulted in a DBTT of -150° C. The DBTT's for the annealed condition and all other aging conditions for Cb-752 were -196° C or lower. Thus, aging embrittlement, as evidenced by at least a 50° C increase in DBTT after aging at 900° C, occurred in Cb-752 in a manner quite similar to the behavior previously observed in Ta-base alloys such as T-111 (refs. 4 and 5).

Results for Mo-TZM are shown in figure 1(d). The DBTT for this alloy in the annealed condition was -15° C. After aging, the DBTT ranged from -15° to 0° C. Aging

at 700°, 825°, and 925° C resulted in a DBTT of -15° C. Aging Mo-TZM at the two higher temperatures, 975° and 1025° C, resulted in a DBTT of 0° C. This slight increase in DBTT is probably not due to the mechanism that produces aging embrittlement in Cb-752 and such Ta alloys as T-111. It may have resulted from an increase in subgrain size or from a redistribution of carbides in the Mo-TZM alloy.

Bend Ductility of Hydrogen-Doped Alloys

The susceptibility of the Cb and Mo alloys to hydrogen embrittlement is of major concern because of the increased sensitivity to hydrogen embrittlement that was observed in Ta-base alloys after long-term aging near 0.4 T_m.

The hydrogen contents and the DBTT results obtained on the hydrogen-doped Cb and Mo alloys of this investigation are summarized in table III. There was a gradual decrease in hydrogen content with an increase in aging temperature for the C-103 alloy. The hydrogen contents of the Cb-1Zr and Cb-752 alloy specimens were independent of aging temperature except for the low hydrogen content of Cb-1Zr aged at 1025° C prior to hydrogen doping. This anomalously low hydrogen content may have arisen because an oxide film prevented hydrogen absorption into the specimen, even though the hydrogen-doping temperature of 825° C was higher than the 815° C which had been used previously for surface "hydrogen activation" (ref. 6). Table III also indicates that the aged Mo-TZM specimens could not be doped with hydrogen. Apparently, long-term aging does not change the low solubility of hydrogen in this alloy.

The effects of hydrogen on the ductility of the four alloys are compared in figure 2. Hydrogen doping to an average content of approximately 60 ppm hydrogen in C-103 (fig. 2(a)) did not affect the ductility at -196° C for specimens in the annealed condition or in any of the aged conditions.

The DBTT of the annealed Cb-1Zr alloy was also below -196° C after doping to an average hydrogen level of approximately 50 ppm. In contrast, the DBTT of all aged and hydrogen-doped Cb-1Zr specimens was -100° C, as illustrated in figure 2(b). A general trend noted in figure 2(b) is that ductility at -196° and -150° C increases with increasing aging temperature. However, hydrogen content was essentially constant for specimens aged at all temperatures and then doped with hydrogen, which suggests that hydrogen variation was not responsible for this ductility behavior. A change in microstructure upon aging may account for this trend in ductility, as discussed in the section General metallography.

The effect of hydrogen doping on the DBTT of Cb-752 is illustrated in figure 2(c). Hydrogen doping to an average level of approximately 40 ppm increased the DBTT of annealed Cb-752 to above room temperature, 50° C. The highest DBTT, 100° C, was

observed for specimens aged at the intermediate aging temperature of 900° C, the temperature at which aging embrittlement occurred in Cb-752.

Attempts to dope Mo-TZM were unsuccessful since a hydrogen content of only 1 ppm resulted for specimens in the annealed or aged conditions. The same range in DBTT, -15° to 0° C, was observed for the specimens after it was attempted to dope them with hydrogen (fig. 2(d)) as was determined for the undoped condition (fig. 1(d)).

All specimens from each of the four alloys were heated in hydrogen at the same time. Therefore, the hydrogen contents given in table III are an indication of the solubility of hydrogen in the four alloys for the time-temperature conditions used for hydrogen doping. The high hydrogen content in the C-103 alloy is attributed to the 10 percent Hf in this alloy. Hafnium increases the solubility of hydrogen in Cb (ref. 6). Compare, for example, the Cb-1Zr alloy, for which a lower hydrogen content resulted from hydrogen doping. In contrast, the 10 percent W in the Cb-752 alloy would be expected to reduce the solubility of hydrogen in Cb as a result of W increasing the alloy electron concentration (refs. 6 and 7). Hydrogen content in this alloy was the lowest for the three Cb alloys. It is well known that hydrogen has a low solubility in Mo alloys. The present results show that long-term aging does not change the solubility of hydrogen in an Mo alloy that contains reactive elements such as Ti and Zr.

Metallographic Examination

General metallography. - The microstructures of C-103, Cb-1Zr, Cb-752, and Mo-TZM samples in the annealed and aged conditions are shown in figures 3 to 6, respectively. Results of grain-size measurements made on these specimens are given in table II. For the C-103 specimens (fig. 3), no apparent change in microstructure occurred as a result of the long-term aging treatment and, as shown in table II, grain size did not change significantly during aging.

The Cb-1Zr alloy (fig. 4) exhibited a change in microstructure with increasing aging temperature. After aging at 700° and 825° C, platelet-type particles, primarily along grain boundaries, are evident in figures 4(b) and (c). After aging at 925° C, the microstructure was characterized by intergranular platelet-type particles, but the grain boundary areas were free of particles (fig. 4(d)). The microstructures of the Cb-1Zr alloy after aging at 975° and 1025° C were free of any particles (figs. 4(e) and (f)). Accompanying the disappearance of the platelet-type particles at grain boundaries was an increase in grain diameter from 20 μm for the annealed material to approximately 28 μm for the three higher aging temperatures (table II). Although these changes in microstructure occurred in the Cb-1Zr specimens, the DBTT remained at or below -196° C for all aging conditions. As noted previously, the ductility of the alloys after hydrogen doping at -196° and -150° C was dependent upon aging temperature (fig. 2(b)). The

presence of the precipitate particles combined with hydrogen may account for the low ductility observed for specimens aged at the lower temperatures. Ductility increased for the higher aging temperatures, which also resulted in the disappearance of the platelet particles (figs. 4(e) and (f)).

Aging the Cb-752 alloy (fig. 5) also resulted in significant microstructural changes. The annealed material and the specimens aged at the two lower temperatures (figs. 5(a) to (c)) were characterized by deformation lines lying parallel to the rolling direction. These lines appear to be continuous across grain boundaries, as shown clearly in the annealed material (fig. 5(a)). Aging at 900° C resulted in a banded microstructure (fig. 5(d)) with precipitate particles decorating the deformation lines that were evident in the annealed material. This microstructure consisted of alternate layers of heavily precipitated regions and precipitate-free regions. This 900° C aging treatment also produced aging embrittlement in this alloy, thus suggesting that embrittlement and precipitation are interrelated. This type of banded microstructure is typical of microstructures previously observed in T-111 (Ta-8W-2Hf) after long-term aging near 1040° C (ref. 4), the temperature which produced aging embrittlement in the T-111 alloy. Aging Cb-752 at a higher temperature (1025° C) resulted in the disappearance of the precipitate regions. After aging at 975° C, a slight trace of the banded microstructure is evident (fig. 5(e)). Aging at 1025° C, however, produced a microstructure (fig. 5(f)) which is quite similar to the initial annealed microstructure. This aging feature is also analogous to the aging response of T-111 (ref. 4). Table II indicates that the grain size of Cb-752 did not change significantly as a result of the aging treatments.

Microstructures of the Mo-TZM specimens shown in figure 6 indicate that aging had very little effect on this alloy. Grains were elongated parallel to the rolling direction in the annealed condition, and this structure persisted even after aging at 1025° C (fig. 6(f)). The grain size (table II) did not change significantly for any of the aging treatments.

Scanning electron microscopy. - Fracture surfaces of the Cb and Mo alloy specimens were examined in a scanning electron microscope. Figures 7 and 8 show fracture surfaces of aged C-103 and Cb-1Zr alloy specimens after testing at -196° C. Since these alloys were ductile in this condition, repeated reverse bending was required to fracture the specimens. Fracture surfaces for both alloys were characterized by ductile tearing, with no indication of grain-boundary separation. Characteristic X-ray analyses of the fractured surfaces are shown in figures 7(b) and 8(b). The peaks for the elements detected are labeled in the figures. In each case the major alloy constituents were identified, that is, Cb and Hf for C-103 (fig. 7(b)) and Cb and Zr for Cb-1Zr (fig. 8(b)).

The fracture surface of a Cb-752 specimen aged at 900° C and subsequently tested at -196° C is shown in figure 9(a). Aging embrittlement, which occurred at this temperature, produced a brittle, intergranular fracture. Particles were observed on the grain-boundary surfaces and at grain-boundary intersections. The analysis of a grain-

boundary surface area that was free of particles is shown in figure 9(b). Only Cb and W were detected in this region. In contrast, analysis of a grain-boundary region that contained a precipitate particle (fig. 9(c)) exhibits Zr peaks in addition to the Cb and W peaks. These results suggest that the particles are Zr rich compared with the surrounding grain-boundary surface. These results are similar to results obtained on tantalum-base alloys containing W and Hf additions, where particles were determined to be Hf rich (refs. 3 to 5).

Scanning electron microscopy results for an Mo-TZM specimen are shown in figure 10. The specimen was tested at -15° C after aging at 975° C and exhibited a bend angle of approximately 60° (fig. 1(d)). The fracture appearance of this specimen reveals a mixed mode of failure involving areas of ductile tearing, transgranular cleavage, and grain-boundary fracture. Only Mo was detected in this specimen by the characteristic X-ray technique (fig. 10(b)).

DISCUSSION

Comparison with Results for Tantalum Alloys

Results of this study have shown that C-103 and Cb-1Zr are not susceptible to aging embrittlement after long-term aging over the homologous temperature range 0.35 to 0.48 T_m. This corresponds to the temperature range for which these alloys are being considered for structural applications in a multihundred-watt, radioisotope-turbogenerator power system. These two alloys were ductile at -196° C under all aging conditions.

A third Cb alloy, Cb-752, exhibited some effects of aging embrittlement after aging at 900° C (or 0.43 T_m). This alloy was included in this study to determine if aging embrittlement in Cb alloys is dependent upon alloy composition, as was shown previously (ref. 5) to be important for Ta alloys. Results on Ta-base alloys showed that grain-boundary segregation of Hf led to aging embrittlement during subsequent testing at room temperature and at -196° C. Hafnium segregation occurred in Ta alloys that contained alloy additions of both W and Hf but did not occur in a binary Ta-2Hf alloy. These results led to the conclusion that W was involved in the Hf segregation problem.

The results of the present study indicate that a similar situation exists in the three Cb alloys investigated. Segregation did not occur in the binary Cb-1Zr alloy, which might be expected to behave similarly to the Ta-2Hf alloy. In addition, Hf segregation did not occur in the C-103 alloy, which contains a high Hf concentration (10 Hf) plus several other minor alloy additions. However, in Cb-752, which contains both W and Zr, grain-boundary Zr segregation occurred and produced about a 50° C increase in the DBTT of this alloy. The mechanism postulated to be responsible for Hf segregation in

Ta-W-Hf alloys was that lattice contraction, which occurs upon adding W to Ta (refs. 8 and 9), causes the larger Hf atoms to segregate to misfit or grain-boundary areas. Competing with this equilibrium segregation process is diffusion, which tends to evenly distribute the solute at higher aging temperatures. Differences in atomic size and changes in the lattice parameter are similar for Ta-W-Hf alloys and the Cb-752 alloy. A lattice contraction occurs upon adding W to Cb. The Zr atom is larger than the Cb or W atoms; therefore, Zr will tend to segregate to misfit regions such as grain boundaries during long-term aging at a critical temperature. For this alloy after 1000 hours of aging, the critical temperature was determined to be 0.43 T_m (900° C). Aging at higher temperatures resulted in ductile behavior and the absence of Zr grain-boundary segregation, apparently because of homogenization by diffusion. In contrast, at temperatures less than 900° C, aging for longer than 1000 hours might cause Zr segregation and aging embrittlement to occur. (Greater aging times compensate for the slower diffusion rates at the lower temperatures.) For example, welded T-111 aged for 100 hours at 980° C had a DBTT below -196° C. However, aging for 10 000 hours at the same temperature increased the DBTT to 50° C (ref. 2).

Aging embrittlement effects on Cb-752 were not as severe as those observed previously for T-111, for which loss of room-temperature ductility was observed (ref. 5). For Ta-base (Ta-W-2Hf) alloys, ductility improved as the W content decreased. On an atomic percent basis, the solute contents in Cb-752 are 5.2W and 2.9Zr. The results for Cb-752 compare more favorably with the Ta-4W-2Hf results of reference 5. Aging embrittlement in these alloys produced brittle failure at -196° C; but at room temperature, aged specimens could be bent 180° with only slight surface cracks. These results indicate that the increase in DBTT as a result of long-term aging at 0.41 to 0.43 T_m may be quite similar in both Cb-base and Ta-base alloys which have equivalent solute additions of W and either Zr or Hf.

Embrittlement from hydrogen doping was most pronounced in the Cb-752 alloy, in which aging embrittlement also occurred. Since the annealed material, as well as all aged specimens, experienced equivalent increases in DBTT, it is not clear from the results of this study that aging increases the sensitivity to hydrogen embrittlement in Cb-752. Rather, it appears that this alloy is highly sensitive to hydrogen embrittlement under all conditions at a hydrogen content of about 40 ppm.

The increase in the DBTT of Cb-1Zr as a result of doping with 50 ppm hydrogen is in agreement with results observed previously on unalloyed Cb (ref. 6). While undoped Cb had a DBTT below -196° C, material doped with 20 ppm hydrogen had a DBTT of -70° C. Apparently, the increased tolerance for hydrogen in C-103 as a result of the Hf addition (ref. 6) mitigates the effect of hydrogen on DBTT in this alloy. Conversely, the reduced tolerance for hydrogen in Cb-752 as a result of the W addition (ref. 7) results in this alloy being more susceptible to hydrogen embrittlement.

It was postulated that the Mo-TZM alloy might also exhibit aging embrittlement and increased sensitivity to hydrogen embrittlement since the alloy contains the reactive elements Ti and Zr. These alloying elements have larger atomic radii than Mo (ref. 10) and may tend to segregate to grain boundaries during long-term aging in a manner analogous to Zr and Hf segregation in Cb and Ta alloys. This phenomenon was not detected in Mo-TZM; consequently, aging embrittlement did not occur in this alloy. Furthermore, since aging did not result in grain-boundary segregation of the reactive elements Ti and Zr, the Mo-TZM alloy could not be doped with hydrogen. Thus, hydrogen embrittlement is not a problem in this alloy even after aging.

Application of Results

The results from the current investigation of Cb alloys and previous studies of Ta alloys (refs. 3 to 5) have established that aging embrittlement can occur as a result of long-term aging near 0.41 to 0.43 T_m in alloys with 4- to 8-atomic-percent W and 2- to 3-atomic-percent Zr or Hf. If the use of alloys with combinations of solutes in this concentration range is proposed for the critical temperature range, extreme care should be taken during subsequent handling after cooldown to room temperature. Although the DBTT of Cb-752 was well below room temperature after aging for 1000 hours, aging for longer times may further increase the DBTT to above room temperature. Great care should also be exercised to prevent exposure to hydrogen. In addition to Cb-752, other Cb alloys that would be expected to be susceptible to aging embrittlement include FS-85 (Cb-27Ta-10W-1Zr), D-43 (Cb-10W-1Zr-0.11C), and C-129Y (Cb-10W-10Hf-0.2Y). Aging embrittlement has been observed in FS-85 and in C-129Y (ref. 2). Data have not been reported on D-43.

Aging embrittlement is not a problem in Mo-TZM and would not be expected to occur in the Mo-0.5Ti alloy.

CONCLUSIONS

Based on a study of the long-term (1000 hr) aging of three columbium (Cb) alloys and a molybdenum (Mo) alloy at temperatures in the range 700° to 1025° C, the following conclusions were drawn:

1. The Cb alloys C-103 and Cb-1Zr and the Mo-TZM alloy are not susceptible to aging embrittlement. Specimens aged over the temperature range 725° to 1025° C for 1000 hours were ductile in bending at -196° C.

2. Aging embrittlement occurs in the Cb-752 alloy as a result of long-term aging at 900° C (0.43 T_m, where T_m is the absolute melting temperature). The ductile-brittle

transition temperature (DBTT) increased from below -196° C to about -150° C after this aging treatment. Aging embrittlement would be expected to occur at lower aging temperatures with increased aging time.

3. A critical combination of tungsten (W) and zirconium (Zr) apparently produces aging embrittlement in Cb-752 in a manner analogous to the production of aging embrittlement in Ta-base alloys containing W and hafnium (Hf) additions. Segregation of Zr to grain boundaries is believed to be promoted by W in the Cb-752 alloy during aging. Subsequent aging embrittlement is characterized by grain-boundary failure at temperatures below the ductile-brittle transition temperature.

4. Post-aging hydrogen embrittlement was most pronounced in the Cb-752 alloy. An increase in DBTT of at least 200° C resulted from doping either annealed or aged specimens with approximately 40 ppm hydrogen. An increase in DBTT of approximately 100° C occurred in aged Cb-1Zr specimens doped with approximately 50 ppm hydrogen. Hydrogen embrittlement did not occur in C-103 doped with approximately 60 ppm hydrogen. Aged Mo-TZM could not be doped with hydrogen.

Lewis Research Center,
National Aeronautics and Space Administration,
Cleveland, Ohio, August 8, 1975,
506-16.

REFERENCES

1. Mini-Brayton Heat Source Assembly Design Study. Vol. 1: Space Shuttle Mission. (GESP-7103-Vol-1, General Electric Co.; NAS3-16810.) NASA CR-121223, 1973.
2. Lessmann, G. G.; and Gold, R. E.: Determination of the Weldability and Elevated Temperature Stability of Refractory Metal Alloys. II - Long-Time Elevated Temperature Stability of Refractory Metal Alloys. NASA CR-1608, 1970.
3. Stephens, J. R.: Role of Hf and Zr in the Hydrogen Embrittlement of Ta and Cb Alloys. Conf. on Hydrogen in Metals: Effects on Properties, Selection, and Design, Am. Soc. for Metals, 1974, pp. 383-392.
4. Watson, Gordon K.; and Stephens, Joseph R.: Effect of Aging at 1040° C (1900° F) on the Ductility and Structure of a Tantalum Alloy, T-111. NASA TN D-6988, 1972.
5. Stephens, Joseph R.: Effects of Alloy Composition in Alleviating Embrittlement Problems Associated with the Tantalum Alloy T-111. NASA TN D-7838, 1975.

6. Chandler, W. T.; and Walter, R. J.: Hydrogen Effects in Refractory Metals. Symp. Metallurgy and Technology of Refractory Metal Alloys, I. Machlin, R. T. Begley, and E. D. Weisert, eds., Plenum Press, 1968, pp. 197-250.

7. Stephens, Joseph R.; and Garlick, Ralph G.: Compatibility of Tantalum, Columbium, and Their Alloys with Hydrogen in Presence of Temperature Gradient. NASA TN D-3546, 1966.

8. Pearson, William B.: A Handbook of Lattice Spacings and Structures of Metals and Alloys. Vol. 1, Pergamon Press, 1958.

9. Pearson, William B.: A Handbook of Lattice Spacings and Structures of Metals and Alloys. Vol. 2, Pergamon Press, 1967.

10. Teatum, E. T.; Gschneider, K. A., Jr.; and Waber, J. T.: Compilation of Calculated Data Useful in Predicting Metallurgical Behavior of the Elements in Binary Alloy Systems. LA-4003, Los Alamos Scientific Lab., 1968.

TABLE I. - VENDOR'S CHEMICAL ANALYSIS OF COLUMBIUM

AND MOLYBDENUM ALLOYS

Alloy	Cb	Mo	Hf	Zr	Ti	Ta	W	C	H	N	O
	Content, wt %							Content, ppm			
C-103	Balance	-------	9.8	0.52	0.95	0.4	0.4	<30	<5	40	130
Cb-1Zr	Balance	-------	---	.95	----	----	---	100	3	70	73
Cb-752	Balance	-------	<.3	<.7	----	<.05	9.8	38	3	100	126
Mo-TZM	-------	Balance	---	.1	.49	----	---	175	4	5	20

TABLE II. - SUMMARY OF AGING TEMPERATURES AND GRAIN

SIZE FOR COLUMBIUM AND MOLYBDENUM ALLOYS

[Aging time, 1000 hr.]

Alloy	Aging temperature, °C	Grain size, μm	Ductile-brittle transition temperature (DBTT), °C
C-103	Annealed for 1 hour at 1345° C	20	<-196
	725	21	
	825	19	
	900	24	
	975	20	
	1025	23	
Cb-1Zr	Annealed for 1 hour at 1345° C	19	<-196
	700	20	
	825	20	
	925	28	
	975	26	
	1025	29	
Cb-752	Annealed for 1 hour at 1345° C	17	<-196
	725	15	<-196
	825	16	<-196
	900	18	-150
	975	14	<-196
	1025	16	<-196
Mo-TZM	Annealed for 1 hour at 1425° C	14	-15
	700	11	
	825	14	
	925	14	
	975	15	0
	1025	14	0

TABLE III. - ANALYSIS OF HYDROGEN-DOPED COLUMBIUM AND MOLYBDENUM ALLOYS

Alloy	Aging temperature, °C	Hydrogen content, ppm by wt		Ductile-brittle transition temperature (DBTT), °C
		As annealed	Hydrogen doped	
C-103	Annealed for 1 hour at 1345° C	0.64	74	<-196
	725		72	
	825		69	
	900		61	
	975		53	
	1025		39	
Cb-1Zr	Annealed for 1 hour at 1345° C	1.2	51	<-196
	700		53	-100
	825		59	
	925		55	
	975		58	
	1025		28	
Cb-752	Annealed for 1 hour at 1345° C	0.45	37	50
	725		37	[a]65
	825		39	[a]70
	900		38	100
	975		40	[a]80
	1025		41	[a]80
Mo-TZM	Annealed for 1 hour at 1425° C	1.2	0.9	-15
	700		1.2	-15
	825		1.7	-15
	925		1.1	-5
	975		1.0	5
	1025		.8	5

[a]Extrapolated values from fig. 2(c).

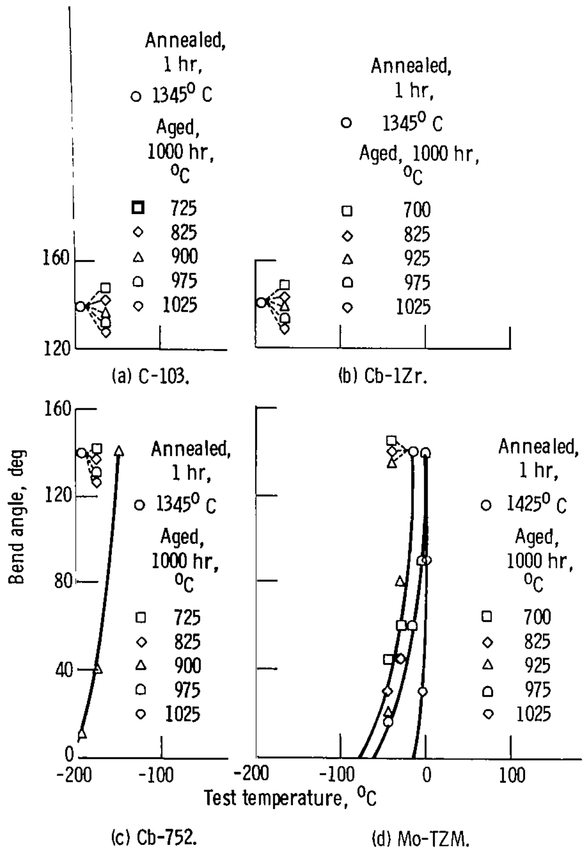

Figure 1. - Effect of aging on the ductile-brittle transition temperature of columbium and molybdenum alloys.

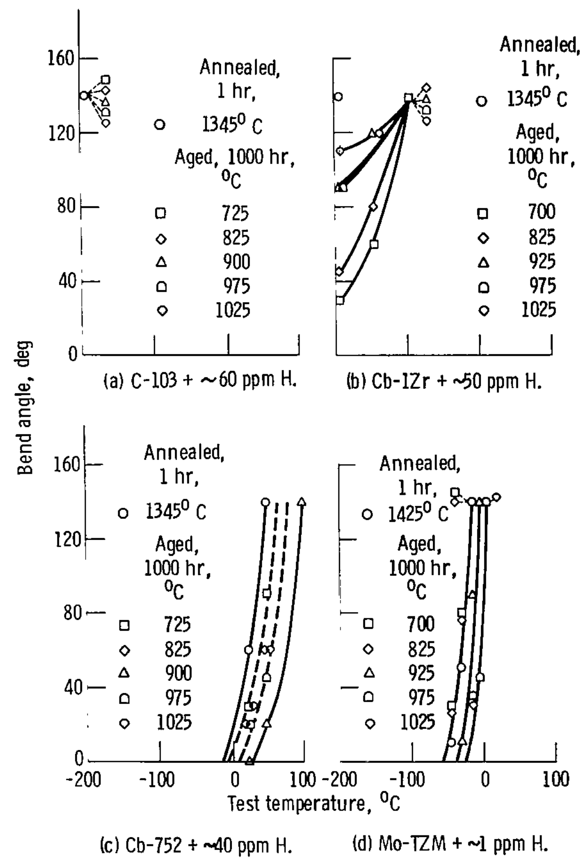

Figure 2. - Effect of hydrogen doping on the ductile-brittle transition temperature of annealed and aged columbium and molybdenum alloys.

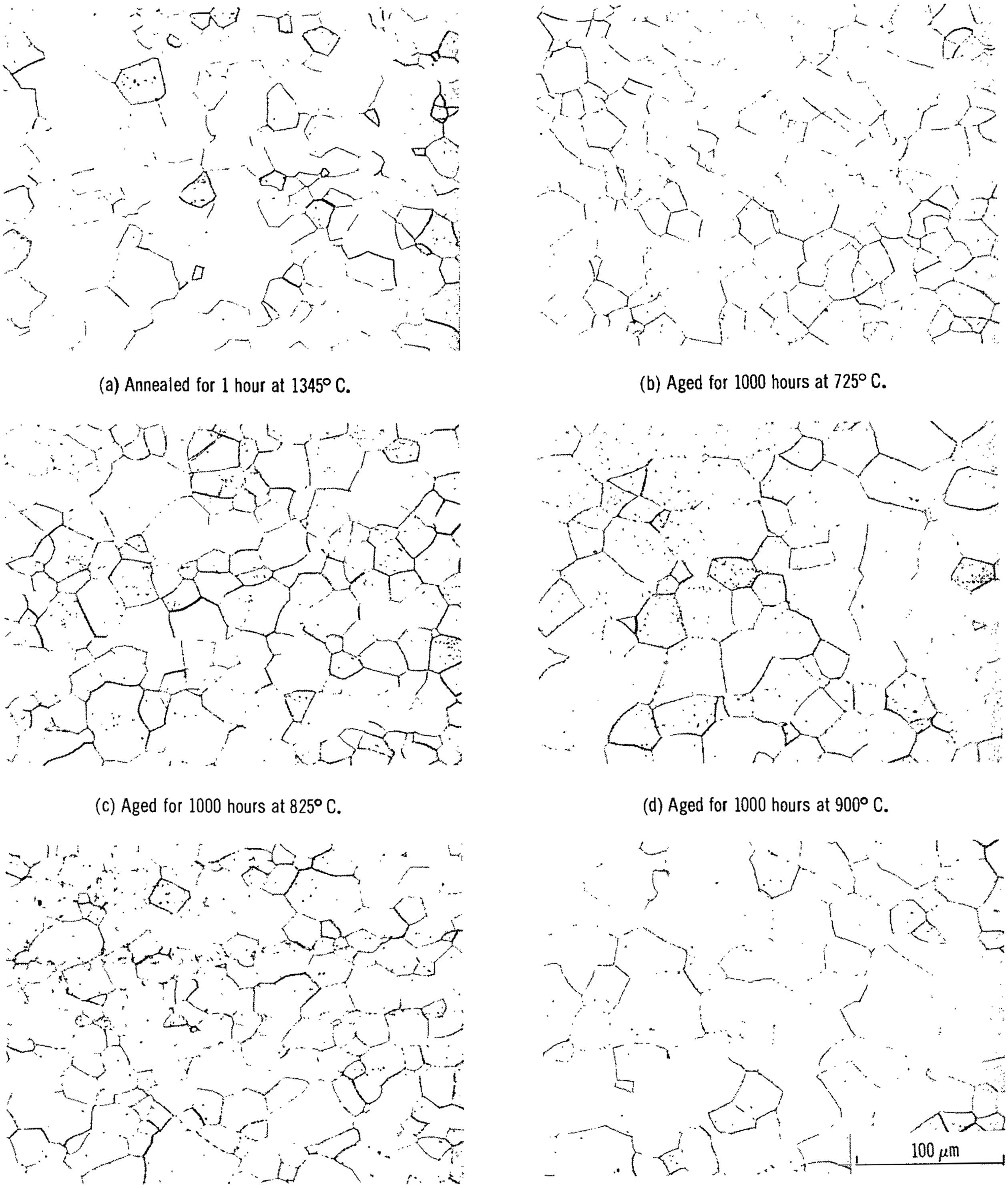

(a) Annealed for 1 hour at 1345° C.

(b) Aged for 1000 hours at 725° C.

(c) Aged for 1000 hours at 825° C.

(d) Aged for 1000 hours at 900° C.

(e) Aged for 1000 hours at 975° C.

(f) Aged for 1000 hours at 1025° C.

Figure 3. - Microstructures of C-103 samples in the annealed and aged conditions. Etchant: ammonium fluoride, nitric acid, and water.

(a) Annealed for 1 hour at 1345° C.

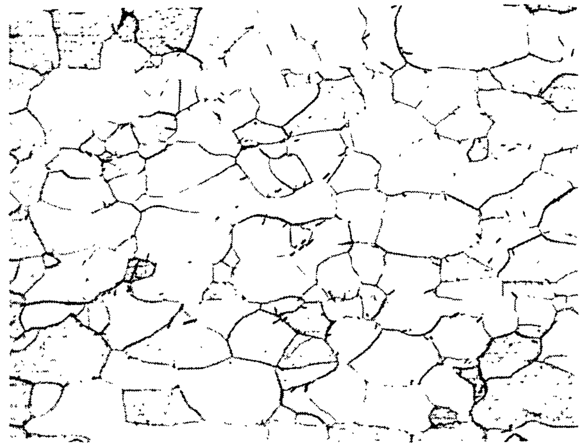

(b) Aged for 1000 hours at 700° C.

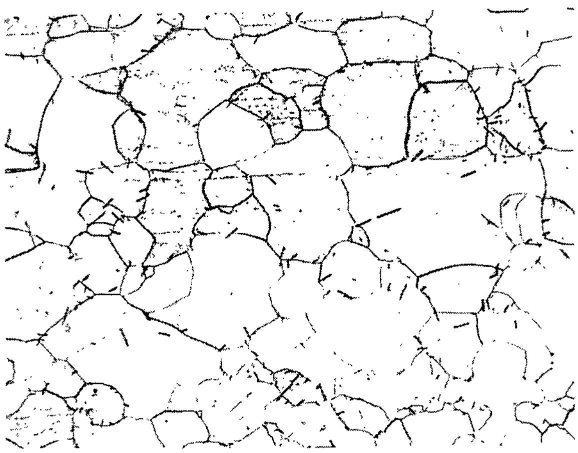

(c) Aged for 1000 hours at 825° C.

(d) Aged for 1000 hours at 925° C.

(e) Aged for 1000 hours at 975° C.

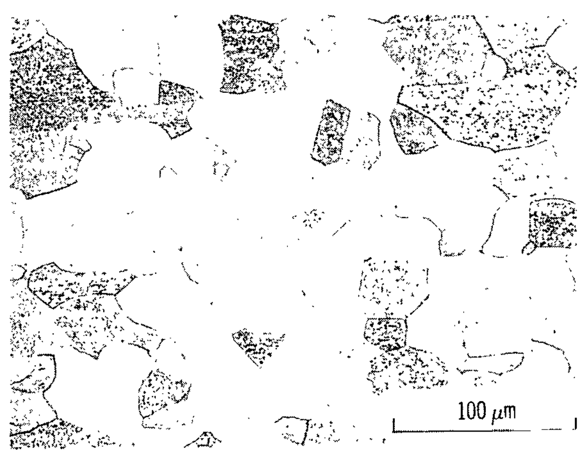

(f) Aged for 1000 hours at 1025° C.

Figure 4. - Microstructures of Cb-1Zr samples in the annealed and aged conditions. Etchant: ammonium fluoride, nitric acid, and water.

(a) Annealed for 1 hour at 1345° C.

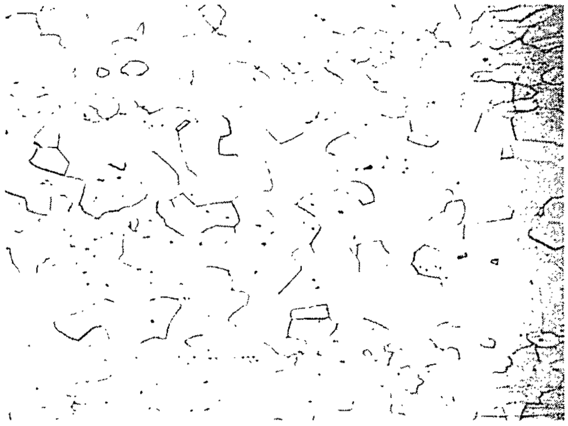

(b) Aged for 1000 hours at 725° C.

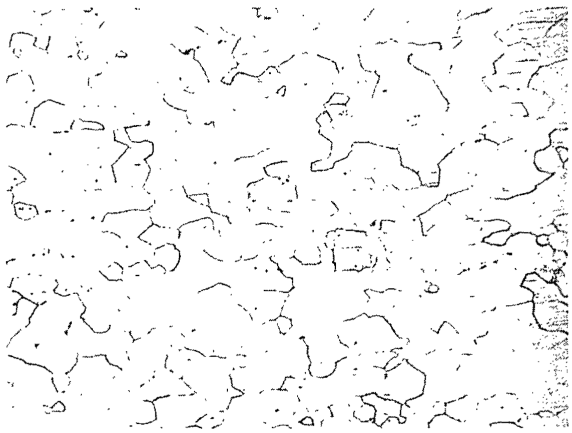

(c) Aged for 1000 hours at 825° C.

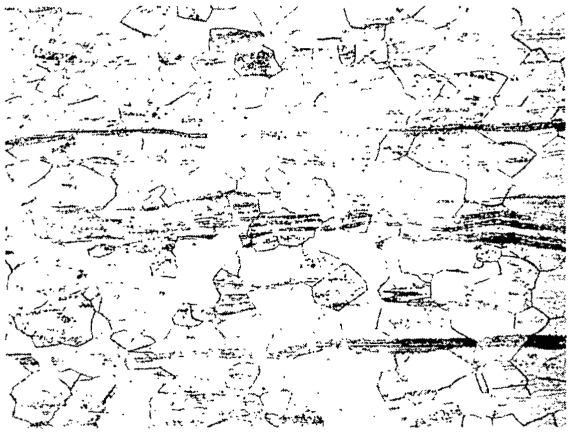

(d) Aged for 1000 hours at 900° C.

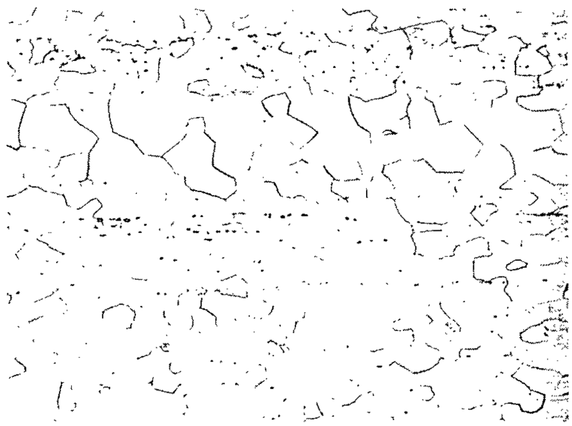

(e) Aged for 1000 hours at 975° C.

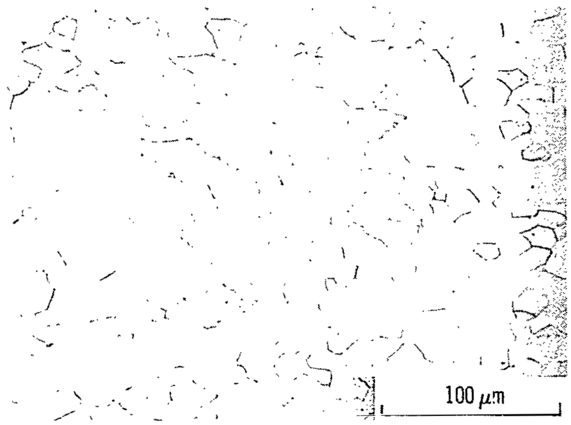

(f) Aged for 1000 hours at 1025° C.

Figure 5. - Microstructures of Cb-752 samples in the annealed and aged conditions. Etchant: ammonium fluoride, nitric acid, and water.

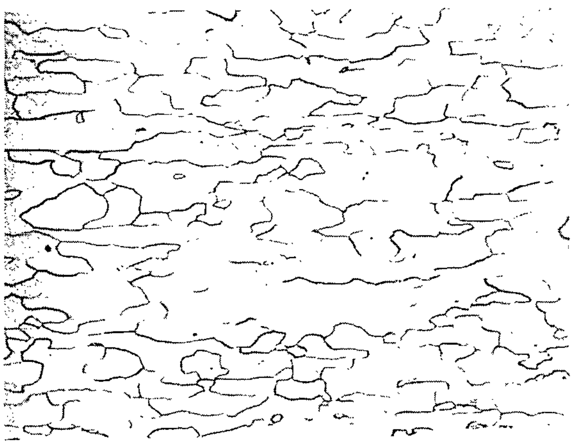

(a) Annealed for 1 hour at 1425° C.

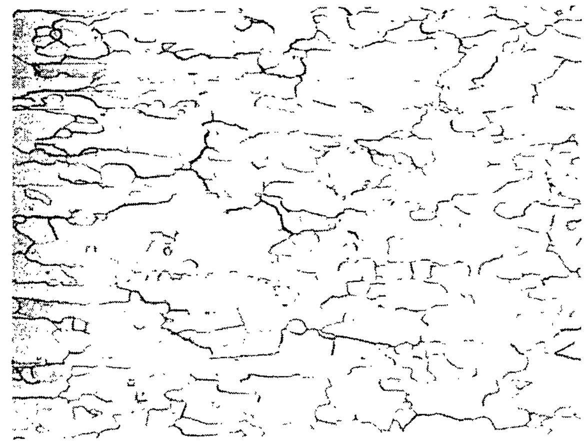

(b) Aged for 1000 hours at 700° C.

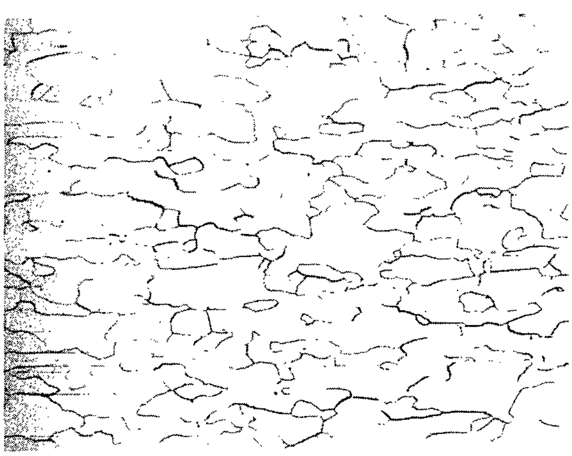

(c) Aged for 1000 hours at 825° C.

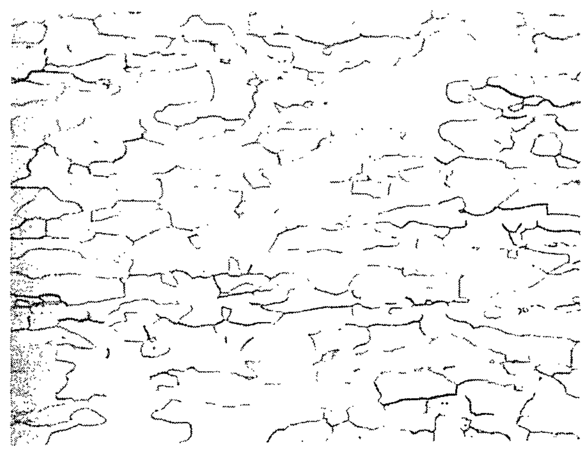

(d) Aged for 1000 hours at 925° C.

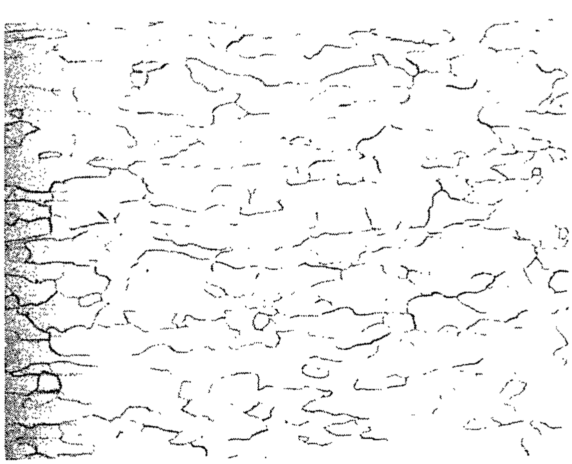

(e) Aged for 1000 hours at 975° C.

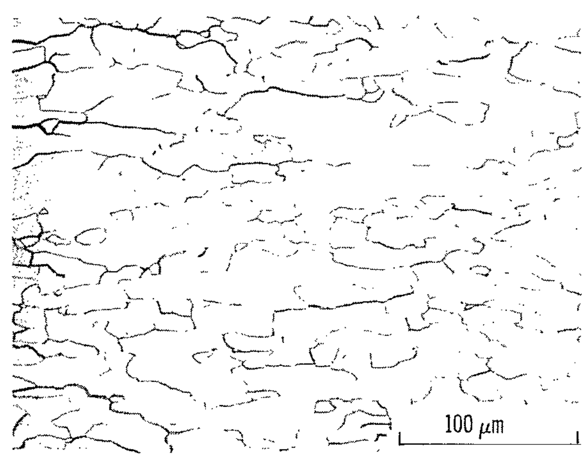

(f) Aged for 1000 hours at 1025° C.

Figure 6. - Microstructures of Mo-TZM samples in the annealed and aged conditions. Etchant: potassium ferrocyanide, potassium hydroxide, and water.

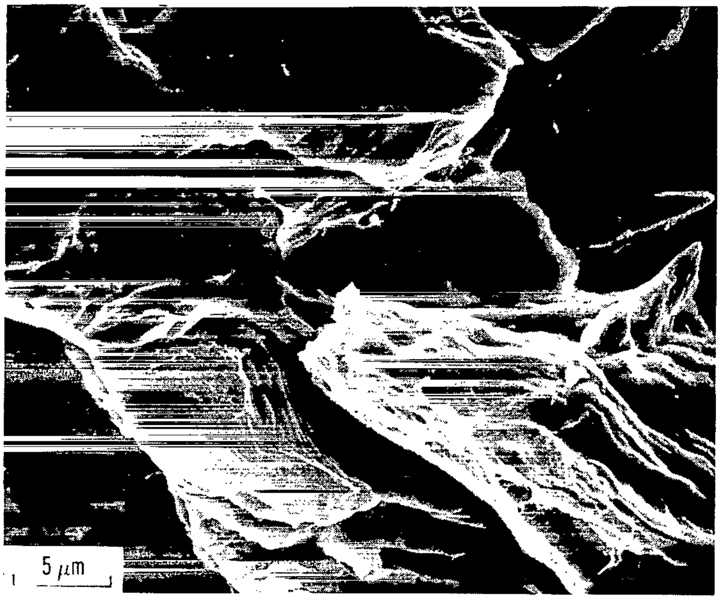

(a) Scanning electron micrograph.

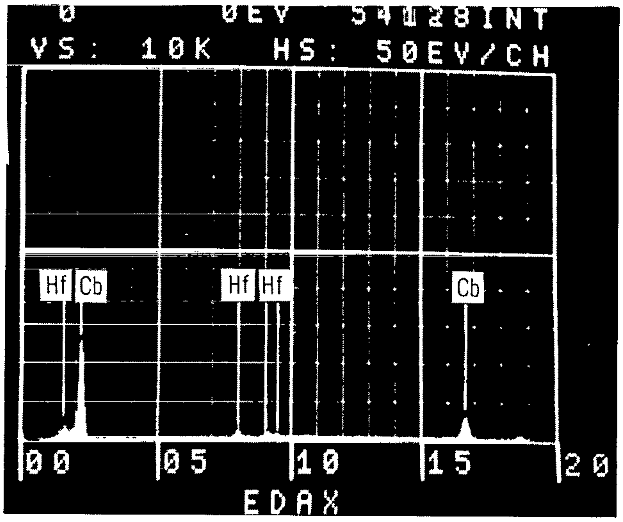

(b) Fracture surface analysis.

Figure 7. - Scanning electron microscope analysis of fracture surface of 825° C aged C-103. Test temperature, −196° C.

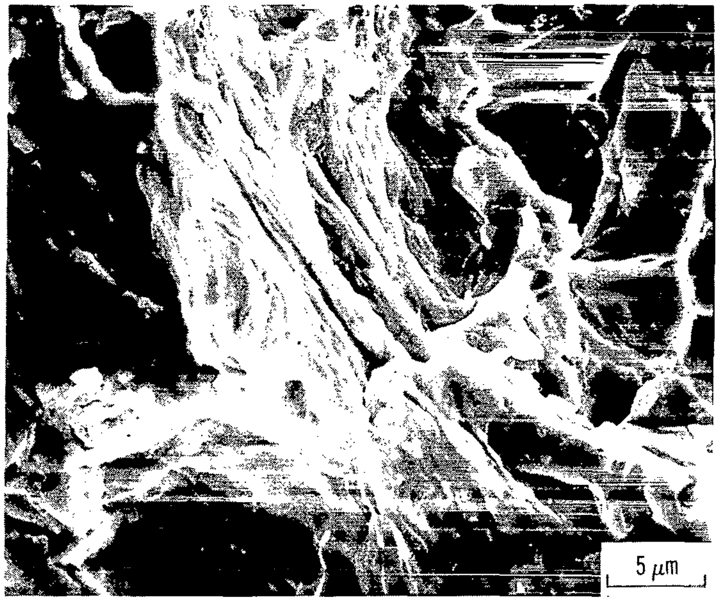

(a) Scanning electron micrograph.

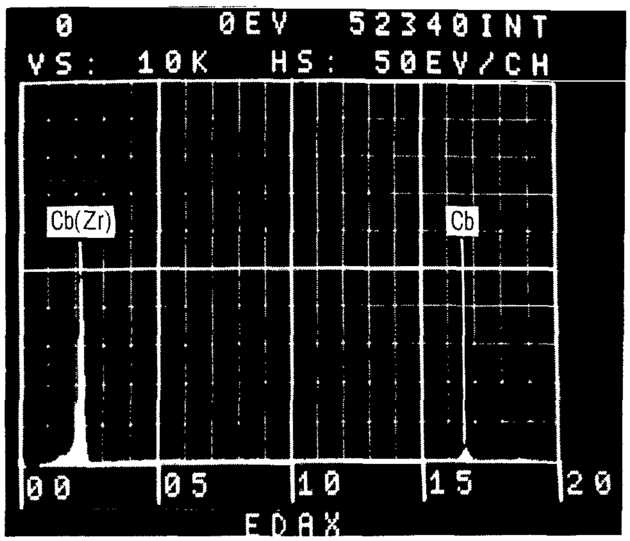

(b) Fracture surface analysis.

Figure 8. - Scanning electron microscope analysis of fracture surface of 700° C aged Cb-1Zr. Test temperature, –196° C.

(a) Scanning electron micrograph.

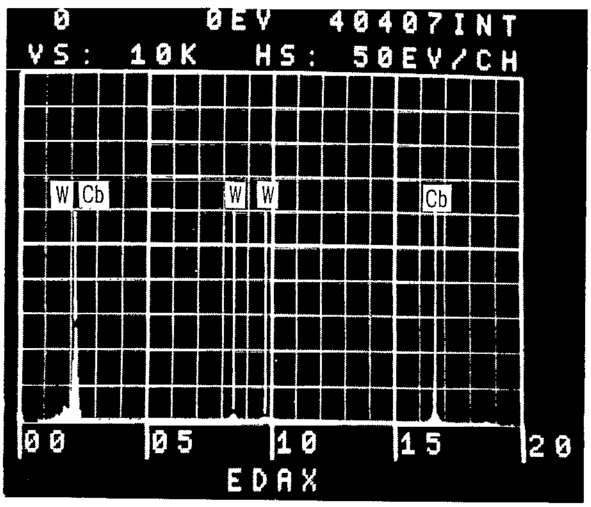

(b) Grain-boundary fracture surface analysis.

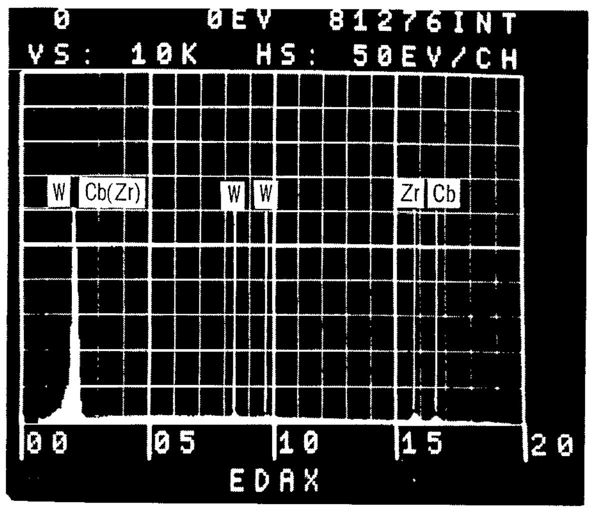

(c) Particle analysis.

Figure 9. - Scanning electron microscope analysis of fracture surface of 900° C aged Cb-752. Test temperature, −196° C.

(a) Scanning electron micrograph.

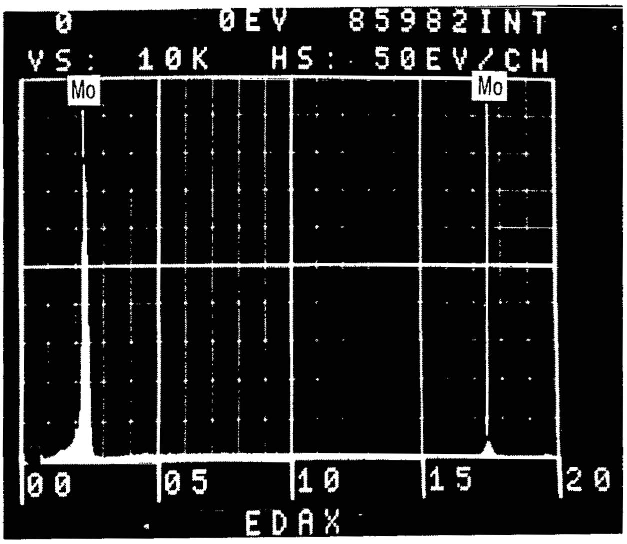

(b) Fracture surface analysis.

Figure 10. - Scanning electron microscope analysis of fracture surface of 975° C aged Mo-TZM. Test temperature, -15° C.

NASA-Langley, 1975 E-8374